Analysis of Protein Separation Mechanism in Charged Ultrafiltration Membrane

Danu Ariono[1], Putu Teta P. Aryanti[2], Anita K. Wardani[1] & I Gede Wenten[1,*]

[1]Chemical Engineering Department, Faculty of Industrial Technology, Institut Teknologi Bandung, Jalan Ganesa 10, Bandung 40132, Indonesia
[2]Chemical Engineering Department, Universitas Jenderal Achmad Yani, Engineering Faculty, Jalan Ter. Jenderal Sudirman, PO BOX 148, Cimahi, Indonesia
*E-mail: igw@che.itb.ac.id

Abstract. The separation mechanism of proteins on a charged ultrafiltration membrane was analyzed using the extended Nernst–Planck (N-P) model. The model was solved numerically based on experimental data during ultrafiltration of bovine serum albumin/BSA and hemoglobin at various pH (between 5 and 8) to obtain the flux parameter (J_v). The flux parameter was used to determine the effective charge of the membrane (ϕ) and the actual membrane porosity (A_k). These two parameters were then used to predict the transport mechanism of proteins through the charged membrane. Higher flux was obtained during the ultrafiltration of BSA compared to hemoglobin. The most effective separation of mixed proteins occurred at pH 5 ($\alpha_{albumin}$ = 5). In addition, the mobility of a single protein was lower than when it was mixed with other proteins that had different charges. The effective charges of the membranes were varied between 0.99996 to 1.0000, which means that the fixed charge on the membrane structure was higher than the concentration of proteins, thus the effective charge of the membrane was not influenced by the presence of protein charge at various pH. On the contrary, the value of A_k was influenced by the type and charge of the proteins. A decrease of negative charge along with an increase of solution pH increased the porosity of the membrane, thus reducing the rejection of proteins.

Keywords: *BSA; charged membrane; Nernst–Planck model; protein separation; ultrafiltration.*

1 Introduction

Membrane-based separation processes have gained an important role in various industrial sectors, including drinking water, chemical, food and beverages, oil and gas, energy, medical and pharmaceutical, and biotechnology [1-9]. Their increasing role is due to interesting features they offer, such as selective separation, relatively low energy consumption, low operating and capital costs, being easy to operate, modularity, having a small foot print, and being simple to scale up [10-13]. In addition, in the case of protein separation, a membrane eliminates the requirement of chemical additives and prevents protein denaturation since the process can be conducted at room temperature [14]. One

Received February 21st, 2018, Revised April 27th, 2018, Accepted for publication May 14th, 2018.
 ISSN: 2337-5779, DOI: 10.5614/j.eng.technol.sci.2018.50.2.4

of the membranes extensively used in protein separation and purification is the polymeric ultrafiltration (UF) membrane. This membrane is designed to provide high retention of proteins while allowing the dissolved contaminants to pass through the membrane.

The protein separation mechanism of UF membranes is based on size (sieving mechanism) and electrostatic charge-effects [15]. In the sieving mechanism, the rejection of solute is determined by the pore size and the pore size distribution of the membrane, which are strongly dependent on the operating parameters, such as solution pH, salt concentration, and system hydrodynamics [16,17]. When the pH of the solution is increased above the isoelectric point (IEP) of the proteins, they become negatively charged and the intramolecular electrostatic repulsion is enhanced. This contributes to the enlargement of the molecular shape, reduces the adsorption of the proteins on the membrane surface, and results in higher rejection [18]. In addition, the intramolecular electrostatic energy is reduced by the increased ionic strength, which leads to enlargement of the proteins [19]. At low ionic strength of the solution, the intramolecular interaction of the proteins is enhanced, which generates a compact protein molecule and increases the amount of adsorbed proteins on the membrane surface [20].

Donnan exclusion is a basic principle that explains the separation mechanism of ions or charged molecules in a charged membrane based on electrostatic interaction or repulsion between both phases. Negatively charged proteins are repelled from the membrane due to the fixed negative charge on the membrane surface [21-23]. The diffusion of ions towards the membrane is generated by a chemical potential gradient ($\Delta\mu$). When the ionic solution is in equilibrium with the ionic membrane, the electrochemical potential (μ) of both phases is equal [24]. The Donnan equation is effective for low concentrations of ions in the feed solution and high concentrations of fixed charges on the membrane surface. In fact, the actual ionic solutions are not in an ideal condition and therefore an activity coefficient needs to be involved to correct for the non-ideality. Numerous empirical models have been developed to calculate the chemical activity of ions in a solution [25-27].

Another basic theory to analyze the transport of proteins through a charged membrane is the Nernst–Planck model, which was developed based on two transport mechanisms, i.e. Fickian diffusion and Faraday ion conduction flux [28]. The Nernst–Planck model not only covers the activity coefficient but also the characteristic parameters of the solution and the membrane. The membrane is assumed to be a thin film that separates two liquid phases and inhibits the diffusion of molecules through the membrane. Further development of the Nernst–Planck model, known as the extended Nernst–Planck model, has been

proposed by introducing a convective transport term in the basic equation [29-31]. To solve the extended Nernst–Planck equation, several parameters need to be assumed or determined from experimental data of single component separation, after which these parameters can be used to predict the separation of a mixed protein solution [30,32].

In this research, the separation mechanisms of two proteins, i.e. bovine serum albumin (BSA) and hemoglobin, were predicted using the extended Nernst–Planck model. The proteins were separated using a sulfonated polyethylene charged membrane. A preliminary experiment was conducted to obtain the empirical data, which were then used to determine the parameters in the Nernst–Planck equation. The separation performance of the proteins was investigated for single-protein and mixed-protein solutions at various pH of the solution. The extended Nernst–Planck model was used to analyze the separation performance and to calculate ion rejection in the single and mixed proteins under various solution pH conditions. The interaction parameters, i.e. effective charge of the membrane and actual membrane porosity, were calculated based on the experimental data during the protein separation process.

2 Extended Nernst–Planck Model

2.1 Separation Mechanism of Proteins on the Charged Membrane

As an amphoteric macromolecule, protein possesses different charges under different solution pH conditions beyond its isoelectric point (IEP) (Figure 1). The behavior of proteins can be traced back to the behavior of ions in the presence of an electric field, thus the Nernst–Planck model can be used to predict the separation mechanism of proteins through membrane charge.

If the membrane thickness is assumed infinite, the diffusion of ions can be assumed to approach a steady state condition and provide a constant junction potential. The transport of ions is driven by the chemical potential ($\Delta\mu_i$) difference, thus the flux of ions at steady state can be expressed in Eq. (1) as follows [24]:

$$J_{i(d)} = \frac{D_i}{RT} C_i \frac{-d\mu_i}{dx} \quad (1)$$

where $J_{i(d)}$ is the flux of ions through the membrane (mol.m^{-2}.h^{-1}), D_i is the diffusion coefficient (m^2.s^{-1}), R is the gas constant (J.mol^{-1}.K^{-1}), T is temperature (K), C_i is the ion concentration in the solution (mol.m^{-3}), and $-d\mu i/dx$ is the gradient in the chemical potential through the membrane thickness, and μi is the chemical potential (J/kg), while x is the membrane thickness (m).

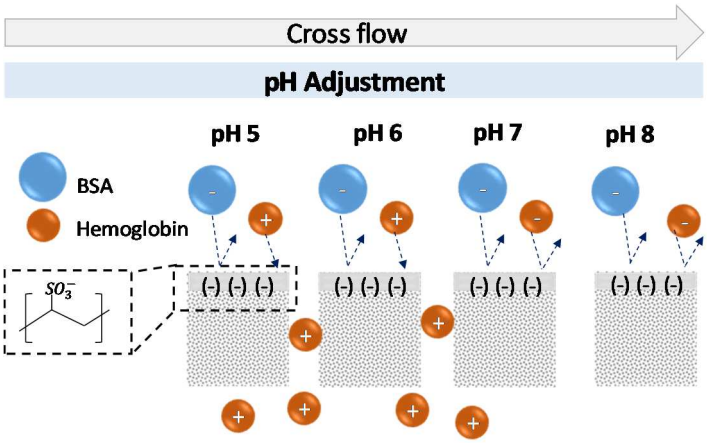

Figure 1 Diffusion of solutes through the charged membrane.

By considering solute activity in the model related to the concentration of ions in the solution, the following equation in Eq. (2) can be used [33]:

$$J_{i(d)} = -D_i C_i \left[\frac{d\ ln\ C_i}{dx} + \frac{d\ ln\ \gamma_i}{dx}\right] = -D_i \left[\frac{dC_i}{dx} + \frac{d\ ln\ \gamma_i}{dx}\right] \quad (2)$$

In an ideal solution, the coefficient activity (γ_i) of component i is equal to one ($\gamma i = 1$).

Diffusion of charged components (ions) through the membrane pores creates an electric field (diffusion potential) that contributes to an additional driving force. The flux induced by an electric field is expressed in Eq. (3) as follows:

$$J_{i(e)} = -u_i z_i C_i (dE/dx) \quad (3)$$

where z_i is the netto molecule charge, or ion valence (ekiv/mol), u_i is ion molar mobility (mol.m^2.J^{-1}.s^{-1}), and dE/dx is the gradient in the electrical potential (in V) through the membrane thickness. For a protein solution, the mobility of the molecules depends on the amount of netto charge and the Faraday constant (F = 96485.332 C mol^{-1}). The total flux resulting from the two types of transport phenomena, i.e. chemical and diffusional potential, is in Eq. (4):

$$J_i = -RTu_i \left[\frac{dC_i}{dx} + C_i \frac{d\ ln\ \gamma_i}{dx} + \frac{z_i C_i}{RT}\frac{dE}{dx}\right] \quad (4)$$

Another type of transport phenomena in the membrane structure is the molecular motion towards the radial pore. The flux of ions due to this motion is $J_{i(c)} = \beta_i C_i J_v$, where β_i is the convective clutch coefficient and J_v is the volumetric flux based on the membrane area [33]. The total flux in the membrane system then becomes:

$$J_i = -RTu_i\left[\frac{dC_i}{dx} + C_i\frac{d\ ln\ \gamma_i}{dx} + \frac{z_iC_i}{RT}\frac{dE}{dx}\right] + \beta_i c_i J_v \quad (5)$$

where c_i is the concentration of component i and Jv is the flux of each component in the membrane system. Eq. (5) is known as the extended Nernst–Planck equation [34], which can be applied to all compounds that move in the membrane system.

2.2 Determination of Effective Charge Fraction (ϕ) and Actual Porosity, A_k, of the Membrane for a Single Protein

During the filtration of proteins, opposite ions will be bounded on the membrane surface due to electrostatic interaction and neutralize the membrane surface charge. In neutral condition, the total molecule netto charges (z_i) will be equal to zero. In addition, the behavior of the ions becomes unideal due to a strong electrostatic interaction between the molecules and the membrane surface. The Donnan equilibrium at the interface between the membrane surface and the external solution is given in Eq. (6) as follows:

$$\left[\frac{\gamma_i c_i}{\gamma_i^o C_i}\right]^{1/z_i} = exp\left[-\frac{F}{RT}\Delta E^D\right] \quad (6)$$

where c_i is the concentration of proteins in the membrane system, C_i is the concentration of proteins in the external solution, and ΔE^D is the Donnan potential in the interface. Kobatake and Kamo used an additive law to calculate the ion activity in electrolyte solution and then developed the Nernst–Planck equation to study the ion transport through a charged membrane [35]. In this study, the additive law was developed for multi-ion systems.

The Nernst–Planck equation for opposite ions is :

$$\frac{dc_i}{dx} = \frac{J_v}{u_1RT}\left[C_1 + \frac{X(1-\emptyset)}{z_i} + C_{1p}\right] - \frac{z_iJ_v}{RT}\left[\frac{(C_1+X/|z_1|)(1-\emptyset)\left[z_1/u_1\left(C_1-C_{1p}+(X/|z_1|)(1-\emptyset)+z_2/u_2\left(C_2-C_{2p}\right)\right)\right]}{z_1^2\left(C_1+X/|z_1|(1-\emptyset)+z_2^2C_2\right)}\right] \quad (7)$$

while for the same ion charge it is :

$$\frac{dc_2}{dx} = \frac{(C_2-C_{2p})J_v}{u_2RT} - \frac{z_2C_2J_v\left(z_1/u_1\left(C_1+X/|z_1|(1-\emptyset)-C_{1p}\right)+z_2/u_2\left(C_2-C_{2p}\right)\right)}{z_1^2\left(C_1+X/|z_1|(1-\emptyset)+z_2^2C_2\right)} \quad (8)$$

Since the membrane thickness is very small, it is assumed that the change in concentration along the membrane thickness is linear (or $dc_i/dx = \Delta c_i/\Delta x$).

Eqs. (7) and (8) are solved numerically by defining C_i as the middle value, $(C_{im} + C_{ip})/2$, to obtain ϕ (dimensionless effective charge of the membrane) and A_k

(actual porosity). C_{im} is the concentration of proteins on the membrane surface, while C_{ip} is concentration of proteins on the permeate side. The actual porosity, A_k, is the ratio between the volumetric flux per unit of pore area and the volumetric flux per unit of membrane area. It has been reported that the fouling phenomena on the membrane system are affected by the A_k value in the membrane system. In this study, the separation mechanism was predicted based on the membrane porosity, A_k, obtained from the modeling based on the separation of proteins at various pH values.

3 Material and Experimental Method

3.1 Materials

In this research, bovine serum albumin (BSA) (Sigma Aldrich, MW 70100, IE point 4.88) and hemoglobin (Sigma Aldrich, MW 66700, IE point 6.79-6.83) were used. The polyethylene membrane was supplied by GDP Filter, Bandung, Indonesia, with an effective diameter of 2.9 cm and equipped with baffles.

3.2 Preparation of Sulfonated Polyethylene UF Membrane

Figure 2 shows a schematic of the polyethylene membrane sulfonation process. The pressure in the equipment system was measured by installing a pressure indicator (PI). 30 %wt of oleum was heated in a boiling flask and the resulting vapor was flowed into a glass tube submerged in an ice bath. The resulting SO_3 was used to sulfonate the commercial polyethylene membrane in an exicator in the presence of dry nitrogen (N_2) gas until the pressure reached 100 mbar (Figure 2). The sulfonation process was carried out for 2 minutes, until the membrane color changed to brown permanently. The exicator was filled with N_2 gas until normal pressure was reached, after which the membrane was taken from the exicator and washed with demineralized water. Finally, the sulfonated membrane was neutralized using NaOH 0.1 N and dried in a dark room. The sulfonated polyethylene membrane had a negative charge due to the formation of aromatic carbon sulfonation.

Before the experiment, the pure water flux (PWF) of the membrane was determined with the following equation in Eq. (9):

$$PWF_{(1)} = \frac{V}{A.t} \tag{9}$$

where PWF_1 is the pure water flux (PWF) ($Lm^{-2}h^{-1}$) before the experiment, V is the volume of permeate (m^3), t is the permeation time (h), and A is the membrane surface area (m^2). After filtration of the protein, the pure water flux was measured using Eq. (10) and symbolized as $PWF_{(2)}$.

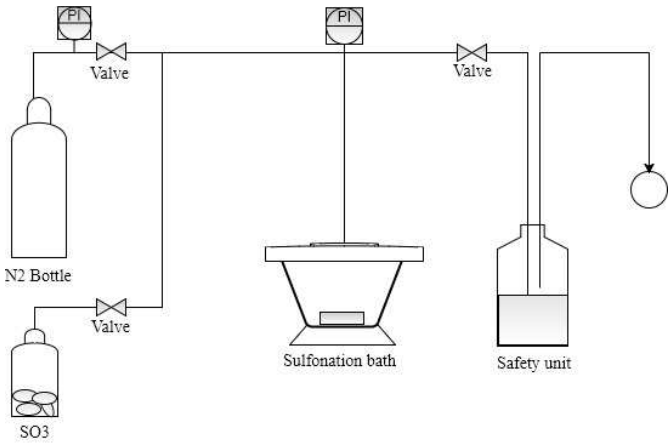

Note: PI is pressure indicator and O is gas release stream

Figure 2 Experimental setup for sulfonation of polyethylene membrane.

3.3 Preliminary Experiment: Protein Separation by Sulfonated UF Membrane

The experimental setup for protein separation with a cross-flow filtration system is shown in Figure 3. A circular flat-sheet membrane with a diameter of 2.9 cm was placed inside the membrane module. The transmembrane pressure (TMP) was varied from 1 to 2.5 bars, after which filtration was carried out at room temperature. The TMP was determined using the following equation in Eq. (10):

$$TMP = \frac{P_f - P_c}{2} - P_p \tag{10}$$

where P_f is the feed pressure (bar), P_c is the concentrate pressure (bar), and P_p is the permeate pressure (bar). The feed tank was immersed in an ice bath to avoid protein denaturation due to the increase in temperature generated by the feed pump. The concentration of proteins in the feed tank was 100 mg/L for the single protein solution and 50/50 mg/L for the mixed protein solution. The pH of the protein solution was varied from 4 to 8. Prior to the experiment, the flux stability of the UF membrane was tested by filtrating demineralized water for 120 minutes at various transmembrane pressures (TMP or ΔP), from 0.5 to 2.5 bar. During the filtration of the proteins, pH adjustment was performed by adding NaOH or HCl to the feed tank. The concentrations of proteins in the permeate and the membrane flux were measured when the steady state condition was reached. In each experiment, the operating conditions (such as temperature, operating pressure, and pH) were kept constant.

3.4 Measurement of Protein Concentration

Five ml of protein solution sample (feed or permeate solution) reacted with 2 ml of specific reagen (ST reagensia). Then the protein concentration was measured by UV-Vis spectrophotometer with 603 nm wavelength for the albumin and 543 nm for the hemoglobin [36,37].

3.5 Charge Density (z) Measurement and Ion Molar Mobility (u)

The charge density of the proteins was measured by acid-base titration. The sulfonated membrane was soaked in 10 mL of HCl 0.0544 N and titrated by NaOH 0.0346 N. The membrane charge (z, in mek/g membrane) was calculated with Eq. (11):

$$z = (B - A)\ x\ eqivalent\ of\ base\ /\ membrane\ weight \quad (11)$$

where A denotes the titrant volume required for 20 ml of acid solution in the absence of a membrane (blank) and B denotes the titrant volume required for 20 ml of acid solution in the presence of a membrane. In this research, the value of A was 15,752 ml, while the value of B was 16,592 ml. The membrane's weight was 0.0056 g. By substituting these values into Eq. (11), the membrane charge was 5.2 mek/g membran.

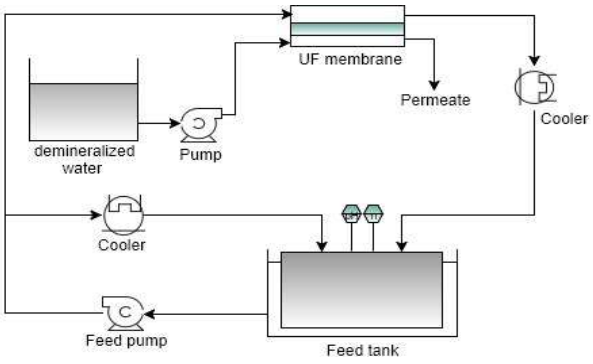

Figure 3 UF membrane unit for protein separation.

In this study, the charge density of BSA was taken from the literature, as shown in Figure 4 [38]. The isoelectric of BSA was found at 4.88. Meanwhile, the charge density of the hemoglobin was measured by acid-base titration from pH 4 to 10 between the IEP of the protein.

The charge density of the hemoglobin (z) was determined based on the mole of the titrant (NaOH 0,012 N, 1000 ppm), which was calculated using the following equation in Eq. (12):

$$z = mole\ of\ titrant\ (NaOH)/mole\ of\ hemoglobin\ at\ IE\ point \quad (12)$$

where the mole of hemoglobin 1000 ppm (50 mL, IE = 7) is 7.496. 10^{-7} mole. The titration data and calculated charge density of hemoglobin are shown in Table 1 and Figure 4. Both proteins showed a decrease in charge density as the solution pH increased or became more negatively charged when the pH of the solution was increased. The ion molar mobility (u_i) was calculated by the Henry equation (Eq. (6)), after which the calculated u_i value was substituted into Eqs. (7) and (8) to calculate the actual membrane porosity (A_k) and ϕ.

Table 1 Titration data and calculated charge density of hemoglobin.

pH	Volume of titrant (mL)	Total volume of solution (mL)	Mole of titrant	Charge, z
3.63	0.000	50.000	2.279 x 10^{-5}	+30
4.23	0.781	50.781	1.342 x 10^{-5}	+18
4.89	1.262	51.262	7.646 x 10^{-6}	+10
6.31	1.658	51.658	2.893 x 10^{-6}	+4
7.00	1.899	51.899	0.000	0
8.40	2.206	52.206	3.958 x 10^{-6}	-5
9.11	2.735	52.735	6.971 x 10^{-6}	-9
9.83	2.905	52.905	1.207 x 10^{-5}	-16

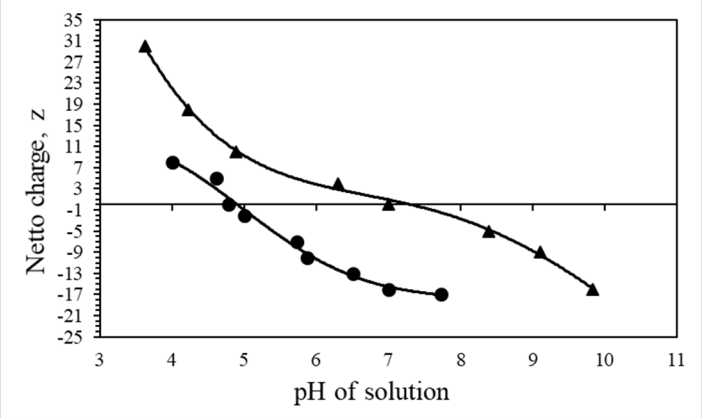

Figure 4 Charge density of single protein at various solution pH: (•) BSA and (▲) hemoglobin.

3.6 Determination of Rejection and Flux of the UF membrane

Rejection of proteins by the UF membrane was calculated using Eqs. (13) & (14) as follows [39]:

$$R_{obs} = 1 - \frac{c_p}{c_f} \quad (13)$$

$$R_r = 1 - \frac{C_p}{C_m} \tag{14}$$

R_{obs} is defined as the capability of the membrane to reject proteins, while R_r is defined as the intrinsic retention that indicates the real (actual) rejection capability of the membrane.

C_m was determined in Eq. (15) as follow:

$$C_m = (C_b - C_p)exp(J_v/k) + C_p \tag{15}$$

The volumetric flux of the UF membrane in steady state condition was determined as in Eqs. (16) and (17) with the following equation [40]:

$$J_v = k\left[ln\frac{R_r}{1-R_r}\right] \tag{16}$$

$$J_v = k\left[ln\frac{C_m - C_p}{C_b - C_p}\right] \tag{17}$$

where k is the mass transfer coefficient of the solute through the membrane pores, which was calculated with Eq. (18):

$$k = {D_i}/{\delta} \tag{18}$$

where δ is the membrane thickness (m), and D_i is the diffusion coefficient of the solutes (cm^2/s). The diffusion coefficient value was calculated using Eq. (19) as follows [41]:

$$D_i = R\,T\,u_i \tag{19}$$

where R is the gas constant (8,314 J/mol), T is temperature (K), and u_i is ion molar mobility. The above flux and mass transfer coefficient are related to the concentration polarization boundary layer.

The mass transfer coefficient of the solutes was determined from a dimensionless number that is related to the hydrodynamic parameters in the membrane system. This is known as the Sherwood number (S_h) expressed in Eq. (20):

$$S_h = {k\,d_h}/{D_i} \tag{20}$$

where d_h is the hydraulic diameter of the membrane pores, which is assumed to be a cylinder or rectangular channel through the membrane thickness. For turbulent flow through a rectangular channel (plate and frame module) the following empirical relationship is given in Eq. (21) [24]:

$$S_h = 0.04\, Re^{0.75} Sc^{0.33} \tag{21}$$

R_e is the Reynold number and S_c is the Schmidt number, which are calculated in Eqs. (22) and (23):

$$R_e = {\rho\, dh\, v}/{\eta} \tag{22}$$

$$S_c = {\eta}/{\rho\, D_i} \tag{23}$$

where v is velocity, η is dynamic viscosity, and ρ is the density of the solution. For a rectangular slit, which has height h and width w, the hydraulic diameter $dh = 2\, w.h/(w+h)$ [24].

4 Results and Discussion

4.1 Protein Separation by Sulfonated Polyethylene UF Membrane

Figure 5 presents the permeate flux during ultrafiltration of single proteins (i.e. BSA and hemoglobin) using a sulfonated polyethylene membrane. Near the IE point of the protein, the permeate flux was slightly lower due to hydrophobic interaction between the protein and the membrane surface. It has been reported that proteins are commonly hydrophobic in neutral conditions and are easily adsorbed in a hydrophobic membrane surface. This behavior leads to fouling formation, which reduces the permeate flux. As shown in Figure 5, a higher permeate flux was obtained during the ultrafiltration of BSA compared to hemoglobin. In addition to having a larger molecule, the BSA charge was more negative than that of the hemoglobin when the solution pH was raised from 4 to 8.

Adsorption of proteins on the membrane surface was decreased due to the electrostatic repulsion between the membrane surface and the proteins, thus higher permeate flux resulted. Conversely, the positive charge of hemoglobin molecules in the range of solution pH generated fouling of proteins on the membrane surface due to strong electrostatic interaction. Fouling on the membrane surface contributes to flux decline during the filtration process.

The real rejection (R_r) and observed rejection (R_{obs}) of the single BSA protein were calculated based on the calculation procedure in Section 3.6. The mass transfer coefficient (k) of the proteins through the membrane was determined based on the Reynold number, the Schmidt number, and the Sherwood number in Eqs. (21) to (24). The calculated k value is shown in Table 2. It shows that an increase of pH increases the mass transfer coefficients of the albumin as well as

the diffusivity, which contributes to a high permeate flux. In contrast to albumin, an increase of the solution pH reduces the mass transfer coefficient and diffusivity of the hemoglobin, which results in a lower permeate flux. A mass transfer coefficient value higher than the diffusivity of the proteins through the membrane pores contributes to the accumulation of proteins on the membrane surface, which leads to the formation of fouling.

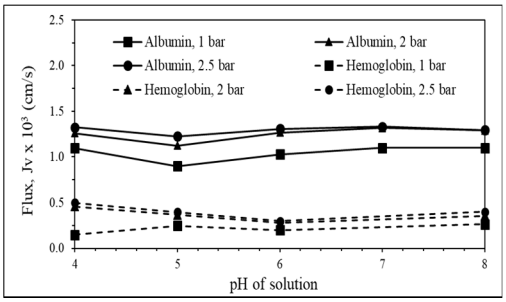

Figure 5 Protein flux on charged polyethylene UF membrane at various pH.

Table 2 Mass transfer coefficient (k) and diffusivity (d_i) of proteins.

pH	Albumin						Hemoglobin					
	1 bar		2 bar		2.5 bar		1 bar		2 bar		2.5 bar	
	$k*e^3$	$Di*e^6$ cm^2/s	$k*e^3$	$Di*e^6$ cm^2/s	$k*e^3$	$Di*e^6$ cm^2/s	$k*e^3$	$Di*e^6$ cm^2/s	$k*e^3$	$Di*e^6$ cm^2/s	$k*e^3$	$Di*e^6$ cm^2/s
4	0.87	0.48	0.52	0.48	0.41	0.48	2.16	1.78	1.27	1.78	0.85	1.78
5	0.48	0.24	0.32	0.24	0.26	0.24	1.58	1.19	0.93	1.19	0.74	1.19
6	1.58	1.20	0.93	1.20	0.93	1.20	0.99	0.59	0.59	0.59	0.63	0.59
7	2.16	1.91	1.26	1.91	1.26	1.91	0.85	0.47	0.50	0.47	0.48	0.47
8	2.13	2.15	1.26	2.15	1.09	2.15	0.70	0.36	0.41	0.36	0.33	0.36

The R_r and R_{obs} values at various operating conditions (1-2.5 bar) and pH of the protein solution are shown in Figure 6. The R_{obs} and R_r were calculated with Eqs. (14) and (15). Since the protein concentration on the membrane surface (C_m) was higher than in the bulk of the solution (C_f), the R_{obs} value was smaller than the R_r value. As shown in Figure 6, the R_{obs} declined around 30% when the solution pH was raised from 4 to 5. As has been explained above, the lowest flux occurred at pH near the IE point, which was caused by protein fouling on the membrane surface due to hydrophobic interaction. A high concentration of proteins on the membrane surface results in a low rejection value.

Increasing the operating pressure from 1 to 2 bar decreased the rejection of the BSA. Higher transmembrane pressure contributed to a higher mass transfer rate

of proteins as well as a higher drag permeation rate, which drove more proteins to the permeate side. When the pH of the solution was further enhanced to the above of IE point, electrostatic repulsion between the membrane surface and the proteins was improved. More than 90% rejection of BSA was achieved at pH 4 and 8. Furthermore, the R_r of BSA decreased up to pH 6 and slightly increased with further increase of solution pH. The high rejection of proteins at high solution pH may be attributed to the enlargement of the molecular shape, becoming close to ellipsoidal. High rejection of BSA was obtained although the operating pressure was increased from 1 to 2 bars.

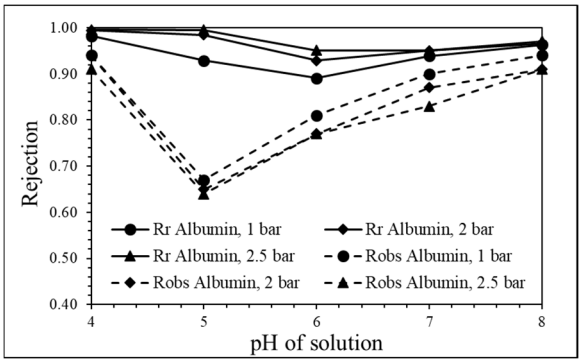

Figure 6 Rejection of BSA at different pH and operating pressures, ΔP.

The real and observed rejection of the hemoglobin at different pH of solution and operating pressures are presented in Figure 7. In contrast to BSA, the rejection of hemoglobin continuously increased by changing the solution pH from 4 to 6 and then became stable with a further increase in pH value. It has been explained that the amount of hemoglobin accumulated on the membrane surface is high in the range of solution pH used. This reduces the effective pore size of the membrane surface and acts as a second membrane layer, which enhances the rejection of proteins.

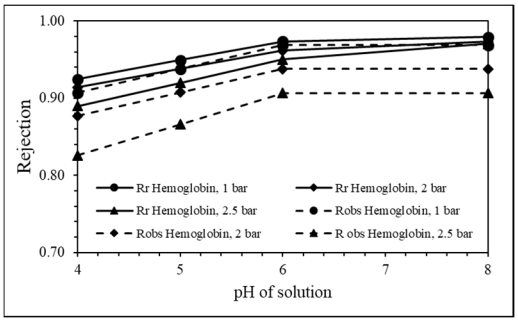

Figure 7 The influence of pH of solution on rejection of proteins.

The role of charge of proteins (z) on flux and R_{obs} for BSA and hemoglobin are shown in Figure 8. The lowest water flux resulted when the charge of the proteins was close to zero or the IE point (Figure 8(a)). Without the surface electric charge, proteins were moved towards to the membrane surface by hydrophobic interaction and formed fouling, which contributed to flux decline. The results show that the surface charge of the proteins plays an important role in the transport of proteins in the membrane system. The influence of the charge density on the permeate flux was similar to the effect on the solute rejection. As shown in Figure 8(b), the rejection of BSA significantly decreased when the surface charge of the proteins was neutral. During hemoglobin separation, the rejection of proteins continuously decreased when the surface charge of the proteins changed to positive. This suggests that the electrostatic interaction between the hemoglobin and the negative charge of the membrane surface contributed to a high accumulation of hemoglobin on the membrane surface, which easily dragged the proteins to the permeate side by cross-flow filtration in the membrane system. However, the overall rejection of hemoglobin was still maintained above 90% with a change in charge or solution pH.

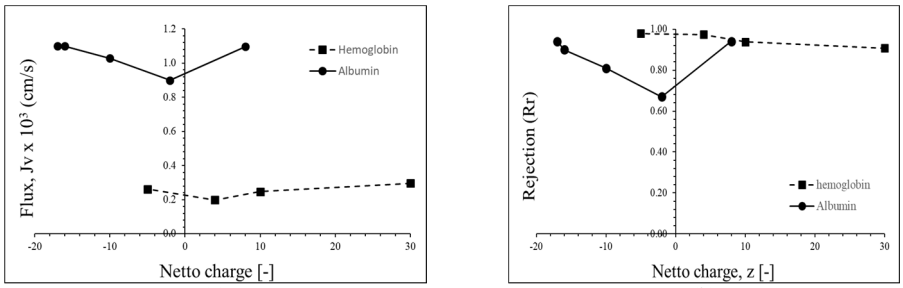

Figure 8 The influence of surface charge on (a) water flux and (b) rejection of proteins.

Figure 9 displays the selectivity during the ultrafiltration of mixed proteins (BSA-hemoglobin at 50/50 mg/l) at varying solution pH and operating pressure. The selectivity of hemoglobin was higher compared to that of BSA at pH 5. As explained in Figures 4 and 5, at pH 5 the charge of BSA was close to neutral (z = -2), while the hemoglobin charge was positive (z = +10). Due to the positive charge value, the hemoglobin molecules were very easily adsorbed on the membrane surface, while the BSA passed to the permeate side. By increasing the operating pressure, the selectivity was decreased due to higher drag permeation of proteins to the permeate side. When the pH was further increased to 7, the selectivity of BSA/hemoglobin was close to zero (α = 0.53-0.66). At this pH, the hemoglobin charge was neutral so, theoretically, the hemoglobin could pass through the membrane pores. However, the presence of positively

charged BSA on the membrane surface provided resistance to the penetration of hemoglobin through the membrane. In addition, the molecular shape of the hemoglobin, similar to an ellipsoid, gave additional resistance to the hemoglobin in passing the membrane pores by the cross-flow mode of filtration.

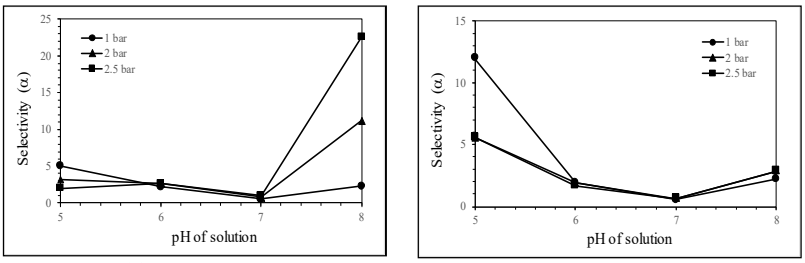

Figure 9 Selectivity of BSA/hemoglobin (50/50 mg/l): (a) based on real rejection (Rr) and (b) based on observed rejection (Robs).

4.2 Ion Molar Mobility (*u*) of Proteins

The mobility of BSA and hemoglobin as single proteins and in a mixed solution during ultrafiltration of proteins are presented in Figure 10(a) and (b). It shows that the mobility of the single proteins decreased when they were in mixed phase. In the single phase, the mobility of the BSA increased with the increase of solution pH, while the mobility of the hemoglobin decreased. During the ultrafiltration of proteins, charge dissociation on the membrane surface depends on the amount of opposite charge of the proteins. As the hemoglobin concentration in the solution increases, the mobility of the proteins decreases due to its interaction with the negatively charged membrane. The influence of the mobility of the proteins in the mixed solution on the permeate flux is shown in Table 3. It shows that the water flux was increased by the increase of solution pH.

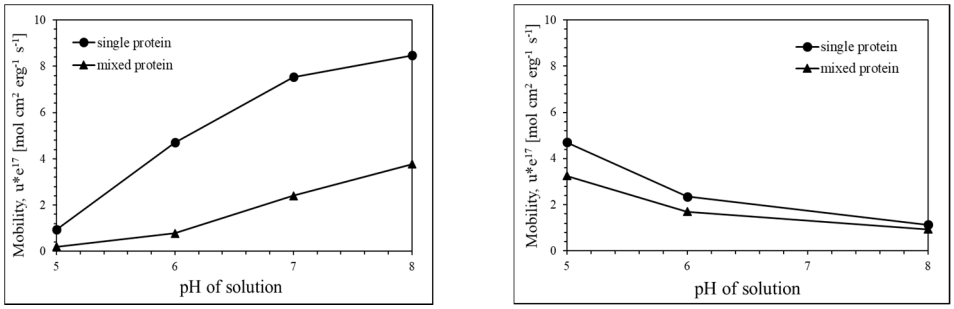

Figure 10 Ion molar mobility of proteins at different pH values: (a) BSA and (b) hemoglobin.

Table 3 Mobility of proteins in mixed solution and its influence on membrane flux.

pH of solution	Mobility in mixed proteins (u_c.e^{17}, mol cm^2 erg^{-1}s^{-1})		Flux (J_v.e^3, cms^{-1})
	BSA	Hemoglobin	
5	0.205	3.25	0.5424
6	0.785	1.70	0.4442
7	2.406	1.32	0.7905
8	3.769	0.94	0.7004

4.3 Effective Charge of Membrane, ϕ, and Membrane Porosity, A_k

The membrane porosity (A_k) was determined based on the J_v value obtained from the numerical calculation of Eqs. (8) and (9). The membrane porosity was calculated by ignoring the polarization concentration; the calculation results are shown in Table 4. It shows that the A_k values were influenced by the type of protein and the charge of the proteins. The A_k value increased with the decrease of the negative charge of the proteins. Apart from the value of J_v, the numerical analysis also resulted in a value of the effective membrane charge, ϕ. It was found that the ϕ values varied between 0.99996 to 1.0000, which indicates that the fixed charge on the membrane structure was higher than the concentration of proteins, thus the ϕ value was not influenced by the presence of charge solute in the solution.

Table 4 Influence of solution pH and pressure on predicted membrane porosity, A_k.

pH	TMP (bar)	Log A_k in single protein solution		A_k in mixed protein solution	
		BSA	Hemoglobin	BSA	Hemoglobin
5	1	-2.62	-0.48	-2.62	-0.49
5	2	-2.73	-0.62	-2.73	-0.62
5	2.5	-2.78	-0.69	-2.81	-0.70
6	1	-5.28	-0.57	-5.27	-0.57
6	2	-5.40	-0.74	-5.40	-0.72
6	2.5	-5.42	-	-5.42	-
7	1	-5.97	-	-5.97	-
7	2	-6.07	-	-6.07	-
7	2.5	-6.11	-	-6.11	-
8	1	-6.19	-2.58	-6.19	-2.57
8	2	-6.20	-2.73	-6.21	-2.75
8	2.5	-6.21	-2.81	-6.21	-2.82

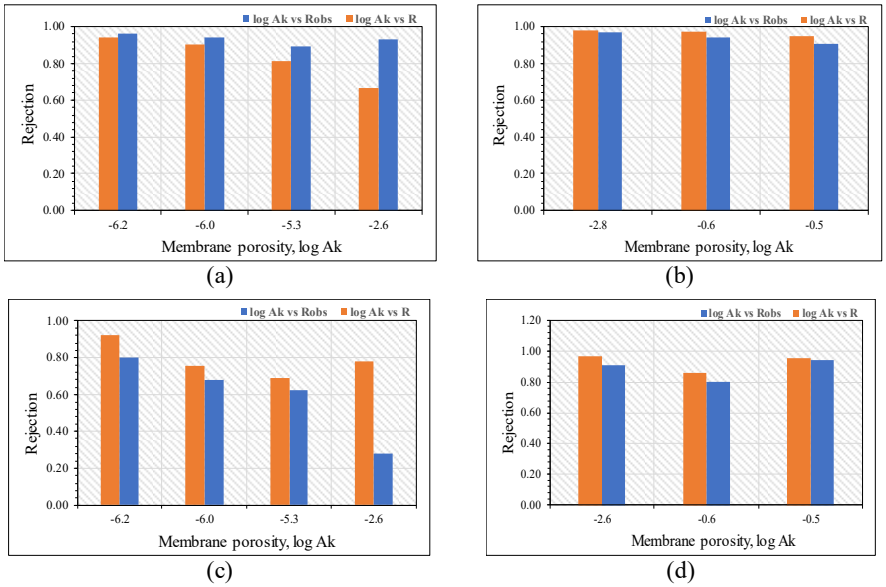

Figure 11 The influence of membrane porosity on rejection of proteins in single protein solution (TMP = 1 bar): (A) BSA, (B) hemoglobin; and in mixed protein solution: (C) BSA, and (D) hemoglobin.

The influence of membrane porosity (A_k) on the rejection of BSA by the sulfonated UF membrane was investigated on a solution containing 100 mg/L of BSA. The increase of solution pH enhanced the membrane porosity, which allowed the BSA to go through the membrane pores to the permeate side. The rejection of BSA was strongly influenced by the solution pH (Figure 11a and 11c). The rejection of BSA slightly decreased when concentration polarization did not occur on the membrane surface due to charge repulsion between the membrane surface and BSA. Meanwhile, the rejection of hemoglobin was not affected by the changes in solution pH (Figure 11B and 11D). The adsorption of hemoglobin on the membrane surface acted as a second layer that inhibited the penetration of proteins through the membrane pores.

5 Conclusion

A protein solution containing bovine serum albumin (BSA) and hemoglobin was separated using a sulfonated polyethylene membrane. The separation process was conducted at various solution pH (between 5 and 8) to investigate the effect of pH on the zeta potential of the proteins and its effect on the separation performance. Experimental data were used to obtain the theoretical permeate flux (J_v) in the extended Nernst–Planck equation. Furthermore, the effective charge of the membrane (ϕ) and actual membrane porosity (A_k) were

determined based on the theoretical permeate flux. These parameters were used to predict the separation mechanism of proteins in a charged UF membrane.

From the experimental data, the UF membrane flux declined near the IE point of the proteins due to the neutral charge of the proteins, which contributed to the adsorption of proteins on the membrane surface by hydrophobic interaction. It was found that higher flux was obtained during the ultrafiltration of BSA compared to hemoglobin. Strong interaction between the positive charge of hemoglobin and the negative charge of the membrane induced fouling formation, which led to a decline of the permeate flux.

The lowest rejection of proteins was achieved when the pH of the solution was near the IE point of the proteins. This is caused by the higher concentration of proteins on the membrane surface. The increase of transmembrane pressure leads to a higher mass transfer rate of proteins and drags the permeation rate, which draws more proteins to the permeate side. The charge of the proteins also influences the selectivity of the mixed proteins during the separation processes. At pH 5, where the BSA was at the IE point and the hemoglobin charge approached +10, while the selectivity of hemoglobin was higher compared to BSA. The positively charged hemoglobin accumulated on the membrane surface while the neutrally charged albumin with a lower molecular weight passed the membrane pores to the permeate side. When the solution pH was increased to 7, the selectivity of BSA/albumin was close to zero (α = 0.53-0.66). This can be attributed to the positive charge of BSA on the membrane surface, which blocks the membrane pores and provides resistance to the penetration of the hemoglobin through the membrane. Effective separation occured at pH 5. In addition, the mobility of the single proteins decreased when they were mixed with other proteins with different charges. When the positive charge of the proteins increased, as found in the hemoglobin solution, the measured mobility of proteins decreased due to neutralization of charges on the membrane surface.

Based on the numerical computation of the extended Nernst–Planck equation it was found that the ϕ values varied from 0.99996 to 1.0000. This indicates that the fixed charge on the membrane structure was higher compared to the concentration of proteins and therefore the ϕ values were not significantly influenced by the presence of charge solute in the solution. In contrast, the actual porosity (A_k) of the membrane was influenced by the type and charge of proteins. The A_k value increased by the decrease of the negative charge of the proteins or the increase of solution pH. When the concentration of solute on the membrane surface was high, the increase of A_k along with the increase of pH reduced the rejection of BSA significantly. This means that the rejection of

BSA was strongly influenced by the solution pH. Meanwhile, hemoglobin rejection was not affected by changes in the solution pH. The decrease of the negative charge along with the increase of the solution pH increased the porosity of the membrane, which then reduced the rejection of proteins.

Acknowledgements

The authors would like to thank the Institut Teknologi Bandung (ITB), Indonesia for its financial support through Program Penelitian, Pengabdian kepada Masyarakat dan Inovasi (P3MI).

References

[1] Drioli, E., Stankiewicz, A.I. & Macedonio, F., *Membrane Engineering in Process Intensification-An Overview,* Journal of Membrane Science, **380**(1), pp. 1-8. 2011

[2] Bernardo, P. & Drioli, E., *Membrane Gas Separation Progresses for process Intensification Strategy in the Petrochemical Industry*, Petroleum Chemistry, **50**(4), pp. 271-282, 2010.

[3] Baker, R.W., *Future Directions of Membrane Gas Separation Technology*, Industrial & Engineering Chemistry Research, **41**(6), pp. 1393-1411, 2002.

[4] Khoiruddin, Aryanti, P.T.P, Hakim, A.N. & Wenten, I.G., *The Role of Ion-exchange Membrane in Energy Conversion*, in AIP Conference Proceedings, AIP Publishing, **1840**(1), 090008, 2017.

[5] Ariono, D., Aryanti, P.T.P., Subagjo, S. & Wenten, I.G., *The Effect of Polymer Concentration on Flux Stability of Polysulfone Membrane*, in AIP Conference Proceedings. AIP Publishing, **1788**, 030048, 2017.

[6] Wardani, A.K., Hakim, A.N., Khoiruddin & Wenten, I.G., *Combined Ultrafiltration-Electrodeionization Technique for Production of High Purity Water*, Water Science and Technology, pp. 2017173, 2017.

[7] Wenten, I.G., Dharmawijaya, P.T., Aryanti, P.T.P., Mukti, R.R. & Khoiruddin, *LTA Zeolite Membranes: Current Progress and Challenges in Pervaporation*, RSC Advances, **7**(47), pp. 29520-29539, 2017.

[8] Sianipar, M., Kim, S.H., Khoiruddin, Iskandar, F. & Wenten, I.G., *Functionalized Carbon Nanotube (CNT) Membrane: Progress and Challenges*. RSC Advances. **7**(81), pp. 51175-51198, 2017.

[9] Mangindaan, D., Khoiruddin, K. & Wenten, I.G., *Beverage Dealcoholization Processes: Past, Present, and Future*, Trends in Food Science & Technology, **71**, 36-45, 2017.

[10] Strathmann, H., *Electrodialysis, a Mature Technology with a Multitude of New Applications*, Desalination, **264**(3), pp. 268-288, 2010.

[11] Aryanti, P.T.P., Sianipar, M., Zunita, M. & Wenten, I.G., *Modified Membrane with Antibacterial Propertie*s, Membrane Water Treatment, **8**(5), pp. 463-481, 2017.

[12] Himma, N.F., Prasetya, N., Anisah, S. & Wenten, I.G., *Superhydrophobic Membrane: Progress in Preparation and its Separation Properties*. Reviews in Chemical Engineering, DOI: 10.1515./revce-2017-0030, 2018.

[13] Purwasasmita, M., Kurnia, D., Mandias, F. Khoiruddin & Wenten, I.G., *Beer Dealcoholization using Non-porous Membrane Distillation.* Food and Bioproducts Processing, **94**, pp. 180-186. 2015.

[14] Saxena, A., Tripathi, B.P., Kumar, M. & Shahi, V.K., *Membrane-based Techniques for the Separation and Purification of Proteins: an Overview*, Advances in Colloid and Interface Science, **145**(1), pp. 1-22, 2009.

[15] Striemer, C.C., Gaborski, T.R., McGrath, J.L. & Fauchet, P.M., *Charge- and Size-based Separation of Macromolecules using Ultrathin Silicon Membranes*, Nature, **445**(7129), pp. 749, 2007.

[16] Xu, Y. & Lebrun, R.E., *Investigation of the Solute Separation by Charged Nanofiltration Membrane: Effect of pH, Ionic Strength and Solute Type*. Journal of Membrane Science, **158**(1), pp. 93-104, 1999.

[17] Ma, J., Qin, L., Zhang, X. & Huang, H., *Temporal Evolution of the Selectivity-permeability Relationship during Porous Membrane Filtration of Protein Solutions*, Journal of Membrane Science, **514**, pp. 385-397, 2016.

[18] Jones, K.L. & O'Melia, C.R., *Protein and Humic Acid Adsorption onto Hydrophilic Membrane Surfaces: Effects of pH and Ionic Strength*, Journal of Membrane Science, **165**(1), pp. 31-46, 2000.

[19] Smith, S.C., Ahmed, F., Gutierrez, K.M. & Rodrigues, D.F., *A Comparative Study of Lysozyme Adsorption with Graphene, Graphene Oxide, and Single-walled Carbon Nanotubes: Potential Environmental Applications*, Chemical Engineering Journal, **240**, pp. 147-154, 2014.

[20] Tercinier, L., Ye, A., Singh, A., Anema, S.G. & Singh, H., *Effects of Ionic Strength, pH and Milk Serum Composition on Adsorption of Milk Proteins on to Hydroxyapatite Particles*, Food Biophysics, **9**(4), pp. 341-348, 2014.

[21] Li, L., Shi, X., Guo, X., Li, H. & Xu, C., *Ionic Protein–lipid Interaction at the Plasma Membrane: What Can the Charge Do?*, Trends in Biochemical Sciences, **39**(3), pp. 130-140, 2014.

[22] Low, S.C., Shaimi, R., Thandaithabany, Y., Lim, J.K., Ahmad, A.L. & Ismail, A., *Electrophoretic Interactions between Nitrocellulose Membranes and Proteins: Biointerface Analysis and Protein Adhesion Properties*, Colloids and Surfaces B: Biointerfaces, **110**, pp. 248-253, 2013

[23] Chakrabarty, T. & Shahi, V.K., *Modified Chitosan-based, pH-responsive Membrane for Protein Separation*, RSC Advances, **4**(95), pp. 53245-53252, 2014.
[24] Mulder, J., *Basic Principles of Membrane Technology*, Springer Science & Business Media, 1996.
[25] Galama, A., Post, J., Stuart, M.C. & Biesheuvel, P., *Validity of the Boltzmann Equation to Describe Donnan Equilibrium at the Membrane–solution Interface*, Journal of Membrane Science, **442**, pp. 131-139, 2013.
[26] Moučka, F., Nezbeda, I. & Smith, W.R., *Chemical Potentials, Activity Coefficients, and Solubility in Aqueous NaCl Solutions: Prediction by Polarizable Force Fields*, Journal of Chemical Theory and Computation, **11**(4), pp. 1756-1764, 2015.
[27] Wei, Z. & Semiat, R., *Applying a Modified Donnan Model to Describe the Surface Complexation of Chromate to Iron Oxyhydroxide Agglomerates with Heteromorphous Pores*, Journal of Colloid and Interface Science, **506**, pp. 66-75, 2017.
[28] Schultz, S.G., *Basic Principles of Membrane Transport*, **2**, CUP Archive, 1980.
[29] Samson, E. & Marchand, J., *Numerical Solution of the Extended Nernst–Planck Model*, Journal of Colloid and Interface Science, **215**(1), pp. 1-8, 1999.
[30] Tsuru, T., Nakao, S-I. & Kimura, S., *Calculation of Ion Rejection by Extended Nernst–Planck Equation with Charged Reverse Osmosis Membranes for Single and Mixed Electrolyte Solutions*, Journal of Chemical Engineering of Japan, **24**(4), pp. 511-517, 1991.
[31] Afonso, M.D. & de Pinho, M.N., *Transport of MgSO4, MgCl2, and Na2SO4 Across an Amphoteric Nanofiltration Membrane*, Journal of Membrane Science, **179**(1), pp. 137-154, 2000.
[32] Bowen, W.R. & Mukhtar, H., *Characterisation and Prediction of Separation Performance of Nanofiltration Membranes*, Journal of Membrane Science, **112**(2), pp. 263-274, 1996.
[33] Dresner, L., *Some Remarks on the Integration of the Extended Nernst–Planck Equations in the Hyperfiltration of Multicomponent Solutions*, Desalination, **10**(1), pp. 27-46, 1972.
[34] Schlögl, R., *Membrane Permeation in Systems Far from Equilibrium,* Berichte der Bunsengesellschaft für physikalische Chemie, **70**(4), pp. 400-414, 1966.
[35] Kobatake, Y. & Kamo, N., *Transport Processes in Charged Membranes*, Prog. Polymer Sci. Japan, **5**, pp. 257-302, 1973.
[36] Bailey, M.P., Rocks, B.F. & Riley, C., *Homogeneous Fluoroimmunoassay Using Lucifer Yellow VS: Determination of Albumin Plasma*, Annals of Clinical Biochemistry, **21**(1), pp. 59-63, 1984.

[37] Warawa, J., Finlay, B.B. & Kenny, B., *Type III secretion-dependent hemolytic activity of enteropathogenic Escherichia coli*, Infection and Immunity, **67**(10), pp. 5538-5540, 1999.
[38] Abramson, H.A., Moyer, L.S. & Gorin, M.H., *Electrophoresis of Proteins and the Chemistry of Cell Surfaces*, Electrophoresis of Proteins and the Chemistry of Cell Surfaces, 1942.
[39] Wang, K.Y. & Chung, T-S., *The Characterization of Flat Composite Nanofiltration Membranes and their Applications in the Separation of Cephalexin*, Journal of Membrane Science, **247**(1), pp. 37-50, 2005.
[40] Hilal, N., Al-Abri, M., Al-Hinai, H. & Abu-Arabi, M., *Characterization and Retention of NF Membranes using PEG, HS and Polyelectrolytes*. Desalination, **221**(1), pp. 284-293, 2008.
[41] Zdunek, A.D. & Selman, J.R., *Mass Transfer and Complexation in Concentrated Zinc/potassium Halide Electrolytes-II*, *Complexation And Migration Effects*, Electrochimica Acta, **34**(10), pp. 1461-1471, 1989.